RSC Advances

PAPER

View Article Online
View Journal | View Issue

Cite this: *RSC Adv.*, 2015, **5**, 84142

Arylhydrazones of barbituric acid: synthesis, coordination ability and catalytic activity of their Co^{II}, $Co^{II/III}$ and Cu^{II} complexes toward peroxidative oxidation of alkanes†

Jessica Palmucci,[ab] Kamran T. Mahmudov,*[ac] M. Fátima C. Guedes da Silva,*[a] Luísa M. D. R. S. Martins,*[ad] Fabio Marchetti,[b] Claudio Pettinari[e] and Armando J. L. Pombeiro*[a]

Received 16th July 2015
Accepted 27th September 2015

DOI: 10.1039/c5ra14078a

www.rsc.org/advances

New *ortho*-substituted arylhydrazones of barbituric acid, 5-(2-(2-hydroxyphenyl)hydrazono) pyrimidine-2,4,6(1*H*,3*H*,5*H*)-trione (H_4L^1) and the sodium salt of 2-(2-(2,4,6-trioxotetra-hydropyrimidin-5(2*H*)-ylidene)hydrazinyl)benzenesulfonic acid (H_4L^2), $[Na(H_3L^2)(\mu\text{-}H_2O)(H_2O)_2]_2$ (**1**), were used in the synthesis of Cu^{II}, Co^{II} and $Co^{II/III}$ complexes, $[Cu(H_2L^1)(H_2O)(im)]\cdot 3H_2O$ (im = imidazole) (**2**), $[Co(H_2O)_6][Co(H_2L^1)_2]_2\cdot 8H_2O$ (**3**), $[Co(H_2L^2)(im)_3]$ (**4**), $[Cu(H_2L^2)(im)_2]\cdot H_2O$ (**5**) and $[Co(H_2O)_6][H_3L^2]_2\cdot 8H_2O$ (**6**). The complexes are water soluble and the mono- or di-deprotonated ligands display different coordination modes, depending on the synthetic conditions. The electrochemical behaviour of all the compounds was investigated by cyclic voltammetry and controlled potential electrolysis, revealing that the ligands are also redox active. All the compounds were evaluated as catalysts for the peroxidative (with H_2O_2) oxidation of cyclohexane at room temperature. The compounds **2** and **3** are the most active ones (yields up to 21% and TON up to 213 are achieved, in the presence of **3**).

Introduction

Barbiturates, besides their biological significance, can also be used as precursors in the synthesis of numerous compounds, such as polymers,[1a] pigments,[1b] dyes[1c] and vitamin B2,[1d] and as building blocks in the construction of supramolecular structures owing to both their H-bond donor and acceptor capabilities.[2] The rich coordination and supramolecular chemistry of barbiturates has been reviewed recently by some of us,[2] but data on the complexes with arylhydrazones of barbituric acid (AHBAs, Scheme 1a) ligands are rather scarce[2,3] and mainly involve copper and zinc complexes.[2,3g,h] All the reported AHBA ligands are stabilized in the hydrazone form with the formation of intramolecular resonance-assisted hydrogen bonding (RAHB)[2] between the hydrazone =N–NH– moiety and a carbonyl group giving a six-membered cycle (Scheme 1a). In order to increase the coordination sites of AHBA ligands, we decided to focus on functionalized forms, in particular the *ortho*-SO_3H and –OH substituted versions (Scheme 1c–d), in view of their promising coordination features. Metallacycles can be obtained and, as shown in related compounds,[4] the *ortho*-SO_3H group can give more stable two six-membered

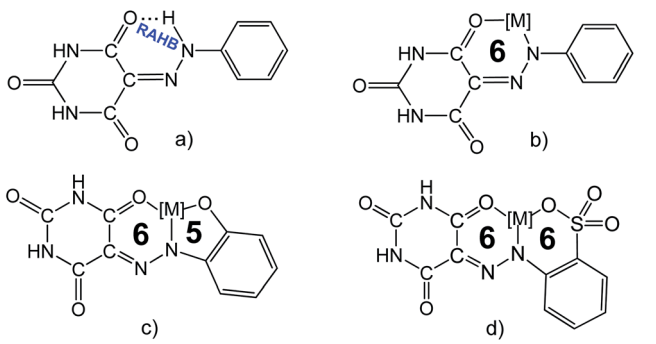

Scheme 1 RAHB in AHBA (a) and expected coordination modes (b–d).

[a]*Centro de Química Estrutural, Instituto Superior Técnico, Universidade de Lisboa, Av. Rovisco Pais, 1049–001 Lisbon, Portugal. E-mail: kamran_chem@mail.ru; kamran_chem@yahoo.com; fatima.guedes@tecnico.ulisboa.pt; lmartins@deq.isel.ipl.pt; pombeiro@tecnico.ulisboa.pt*

[b]*School of Science and Technology, University of Camerino, Chemistry Section, via S. Agostino 1, 62032 Camerino, Italy*

[c]*Department of Chemistry, Baku State University, Z. Xalilov Str. 23, Az 1148 Baku, Azerbaijan*

[d]*Chemical Engineering Department, Instituto Superior de Engenharia de Lisboa, Instituto Politécnico de Lisboa, R. Conselheiro Emídio Navarro, 1959-007 Lisboa, Portugal*

[e]*School of Pharmacy, University of Camerino, Chemistry Section, via S. Agostino 1, 62032 Camerino, Italy*

† Electronic supplementary information (ESI) available: Crystal data, experimental parameters and selected details of the refinement calculations, cyclic voltammogram (for H_4L^1 and **1–3**) and electron absorption spectra of compounds **1–6**. CCDC 1055317, 1055319–1055322 and 1055325. For ESI and crystallographic data in CIF or other electronic format see DOI: 10.1039/c5ra14078a

metallacycles than the matallacycles associated to the *ortho*-OH and to the unsubstituted AHBA ligands (Scheme 1b–d). Moreover, functionalization of a ligand with an hydrophilic polar group, such as –OH, $-SO_3H$, is a common way to increase the water solubility of its complexes, which is important for catalysis in aqueous medium.[4,5]

From other perspective, due to proton-donor or -acceptor sites of imidazole (im), it has been used as an auxiliary ligand or deprotonating agent in the synthesis and design of water soluble coordination compounds.[4] Thus, the use of im as an auxiliary ligand or a deprotonating agent for the weakening/destroying RAHB system in the complexation of AHBA ligands with transition metals such as Cu^{II}, Co^{II}, *etc.* is of practical importance for the development of new synthetic methods.

No application in catalysis of any metal complex of AHBA had been reported so far. Thus, the preparation and characterization of the first Co^{II} and $Co^{II/III}$ complexes, as well as of Cu^{II}, are of significant interest due to, *e.g.*, their possible catalytic applications in the peroxidative oxidation of alkanes, for instance cyclohexane. Thus, another main aim of the current work concerns the extension of the application of AHBA complexes to this field, *i.e.* oxidative catalysis. The partial oxidation of cyclohexane is the main industrial route to cyclohexanone and cyclohexanol, which are important intermediates in the production of adipic acid and caprolactam, also used in the manufacture of nylon-6 and nylon-66 polymers.[6] However, the industrial aerobic oxidation of cyclohexane to the alcohol/ketone mixture, catalysed by Co salts, requires the use of considerable temperature (150–170 °C) and proceeds with a low yield (~4%) in order to achieve a selectivity of *ca.* 85%.[6h,k] Hence, it is of a great practical interest to develop a more efficient, as well as easily synthesizable catalyst for the selective cyclohexane oxidation process able to operate under milder conditions. In addition, such catalyst should be active in a reaction medium that employs either hydrogen peroxide or preferably dioxygen to become an attractive alternative to the currently used industrial processes.

Thus, in this work we focused on the following aims: (i) synthesis of new water soluble AHBA ligands bearing *ortho* -OH and $-SO_3H$ groups, namely 5-(2-(2-hydroxyphenyl)hydrazono)-pyrimidine-2,4,6(1*H*,3*H*,5*H*)-trione ($\mathbf{H_4L^1}$) and sodium salt of 2-(2-(2,4,6-trioxotetrahydro-pyrimidin-5(2*H*)-ylidene)hydrazinyl)-benzenesulfonic acid ($\mathbf{H_4L^2}$), and their application in the preparation of new water soluble Co^{II}, $Co^{II/III}$ and Cu^{II}-AHBA complexes; (ii) study of the physicochemical and electrochemical properties of the ligands and complexes; (iii) application of the complexes as catalyst precursors for the peroxidative oxidation of cyclohexane in aqueous acetonitrile medium, under mild conditions.

Results and discussion

Synthesis and characterization of H_4L^1, Na^I salt and Co^{II}, $Co^{II/III}$ and Cu^{II} complexes

The new AHBAs, namely 5-(2-(2-hydroxyphenyl)hydrazono)-pyrimidine-2,4,6(1*H*,3*H*,5*H*)-trione ($\mathbf{H_4L^1}$) and sodium salt of 2-(2-(2,4,6-trioxotetrahydropyrimidin-5(2*H*)-ylidene)hydrazinyl)-benzenesulfonic acid ($\mathbf{H_4L^2}$), $[Na(H_3L^2)(\mu\text{-}H_2O)(H_2O)_2]_2$ (**1**), were prepared by a modified known[7] aqueous diazotization of 2-aminophenol and 2-aminobenzenesulfonic acid and subsequent coupling with barbituric acid in basic medium, respectively (Scheme 2). $\mathbf{H_4L^1}$ and **1** are highly soluble in DMSO, DMF, water, methanol, acetone and acetonitrile. Both compounds are stabilized in DMSO-d_6 solution in the hydrazone form, as reported analogues.[2,7d] In fact, ^{1}H-NMR spectra of $\mathbf{H_4L^1}$ and **1** in DMSO-d_6 solution at room temperature show only one signal at δ 14.44 and 14.80, respectively, assigned to the proton of the protonated nitrogen atom adjacent to the aryl unit (=N–NH–

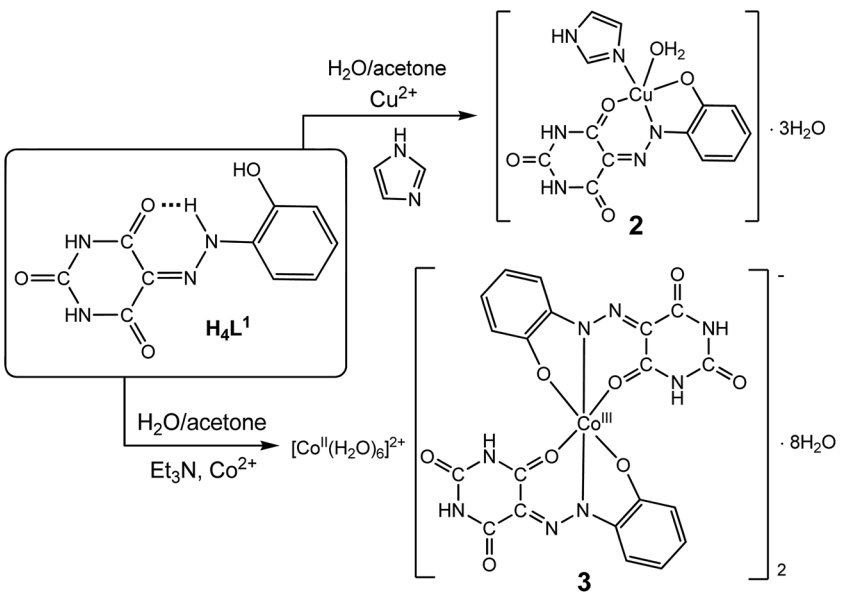

Scheme 2 Synthesis of **2** and **3**.

hydrazone form). In accord, two peaks of the carbonyl groups in the ^{13}C NMR spectra (see Experimental) indicate that one of these groups undergoes a shift due to hydrogen bonding of the carbonyl moiety with the hydrazone NH group. This is in agreement with the low field chemical shift (14.44 and 14.80 ppm) of the hydrazone NH proton and is also consistent with IR data: the stretching bands ν(C=O) and ν(C=O···H) are at 1697 and 1643 (for $\mathbf{H_4L^1}$), 1677 and 1604 (for **1**) cm^{-1}, respectively, the latter being shifted on account of the H-bond.[2,7d] Elemental analysis and the ESI-MS peaks at 249.2 $[Mr + H]^+$ and 702.1 $[Mr - 4H_2O + H]^+$ support the formulation of $\mathbf{H_4L^1}$ and **1**, respectively (Fig. 1S and 2S†). Moreover, X-ray diffraction analysis of **1** is demonstrate that it is stabilized in the hydrazone form (see below).

Reaction of $\mathbf{H_4L^1}$ with Cu^{II} or Co^{II} (nitrate salts) in the presence of imidazole (im) and triethylamine (Et_3N) in acetone–water mixture (4 : 1, v/v) lead to $[Cu(H_2L^1)(H_2O)(im)]\cdot 3H_2O$ (**2**) and $[Co(H_2O)_6][Co(H_2L^1)_2]_2\cdot 8H_2O$ (**3**), respectively (Scheme 2, see Experimental for details). The added base (im or Et_3N) conceivably weakens the hydrogen-bonded system in $\mathbf{H_4L^1}$ and its reactivity increases towards N–H deprotonation and coordination to the metal ions. Both complexes are characterized by elemental analysis, ESI-MS spectra, IR spectroscopy and single crystal X-ray diffraction (see below). In the IR spectra of **2** and **3**, the ν(C=O) and ν(C=N) signals appear at 1714 and 1586, 1719 and 1594 cm^{-1}, respectively, values that are significantly shifted in relation to the corresponding signals of $\mathbf{H_4L^1}$ (1731 and 1697 ν(C=O), 1597 ν(C=N)). Mass spectrometry of **2** and **3** dissolved in methanol shows parent peaks at m/z = 310.7 $[C_{10}H_6CuN_4O_4 + H]^+$ (for **2**) and 167.0 $[Co(H_2O)_6]^{2+}$, 551.2 $[C_{20}H_{12}CoN_8O_8]^-$ (for **3**) (Fig. 3S and 4S†). Elemental analyses are also in agreement with the proposed formulations, which are also supported by X-ray crystallography.

Reactions of $Co(NO_3)_2\cdot 6H_2O$ and $Cu(NO_3)_2\cdot 2.5H_2O$ with **1** in water–acetone mixture (1/3, v/v), in the presence of im led to the Co^{II} and Cu^{II} complexes $[Co(H_2L^2)(im)_3]$ (**4**) and $[Cu(H_2L^2)(im)_2]\cdot H_2O$ (**5**), respectively (Scheme 3). The Co^{II} salt of AHBA, $[Co(H_2O)_6][H_3L^2]_2\cdot 8H_2O$ (**6**), was obtained by mixing (stirring for 10 min) of an acetone–water mixture (4 : 1, v/v) solution of **1**, Et_3N and $Co(NO_3)_2\cdot 6H_2O$ at 80 °C (Scheme 3).

All the isolated compounds, **4–6**, were characterized by elemental analysis, ESI-MS, IR spectroscopy and single crystal X-ray diffraction. In the IR spectra of **4**, **5** and **6**, the ν(C=O) signal appears at 1664, 1633 and 1675 cm^{-1}, respectively, values that are significantly shifted in relation to the corresponding signal of **1** (1677 cm^{-1}). The ESI mass spectra of **4**, **5** and **6** dissolved in CH_3OH show the peaks at m/z = 574.0 $[\{Co(im)_3H_2L^2\} + H]^+$, 510.0 $[\{[Cu(im)_2H_2L^2]\cdot H_2O\} - H_2O + H]^+$, and 682.1 $[Co(H_3L^2)_2 + H]^+$ (Fig. 5S–7S†). Elemental analyses are consistent with the proposed formulations which are also supported by X-ray crystallography (see below). All the obtained complexes are soluble in water, methanol, DMF and DMSO, but later one is the best solvent for them.

The wavelength (λ_{max}) and molar absorption values (ε) of all compounds in the UV-vis region 200–700 nm have been recorded in water solution (Table 1S and Fig. 8S†). In the spectra of $\mathbf{H_4L^1}$ and **1–6** the bands at 234–270 nm are due to π–π^* electronic transition, while the bands at 352–482 nm are mainly of n–π^* type.[7b]

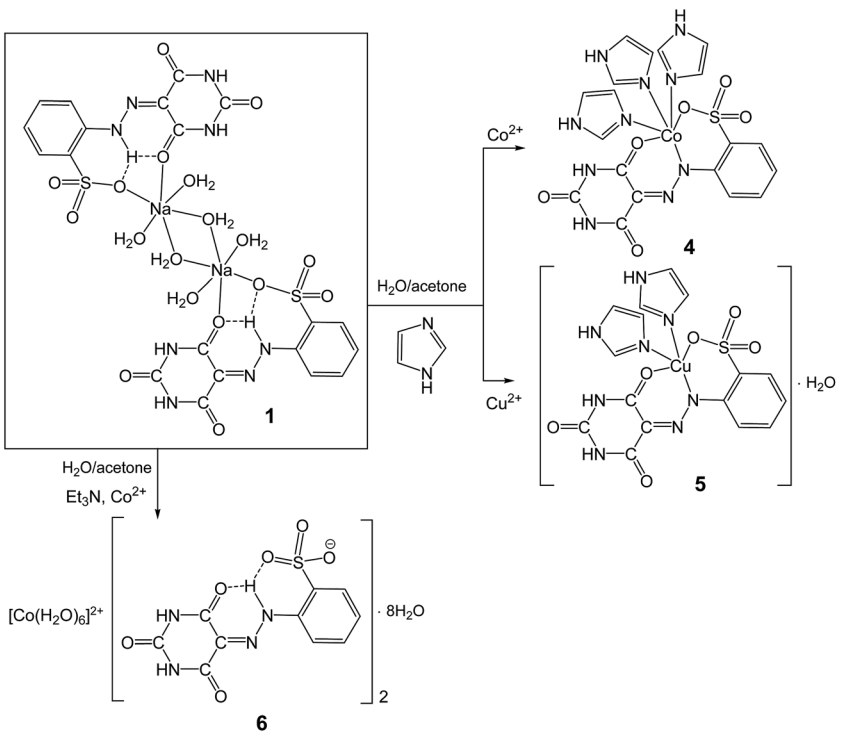

Scheme 3 Synthesis of **4–6**.

X-ray diffraction analyses

Crystals of **1–6** suitable for X-ray diffraction analysis were obtained upon crystallization from water–acetone mixtures (1 : 4, v/v) (the schematic representations of their formulae are shown in Schemes 2 and 3). The structure of **1** (Fig. 9S, ESI†) will not be discussed since it is a preliminary one (78% completeness) and no further suitable crystals of the compound were obtained. Representative plots of **2–6** are depicted in Fig. 1. Crystallographic data and refinement parameters are given in Tables 2S and 3S† H-contacts for **2–6** are outlined in Table 4S† and depicted in Fig. 10S†).

General aspects of the structures. In compound **7** the L^n species cocrystallized with hexaaquacobaltate cation, apart from water molecules, and can be roughly planar as measured by the angles between the least square plane of the heteronuclear ring (plane H) and the least square plane of the phenyl ring (plane P; Table 4S†).

In the mononuclear structures **2–5** an *N*-hydrazone atom, a phenoxyl (in **2** and **3**) or a sulfonyl (in **4** and **5**) O-atom and an additional O-atom from the pyrimidine trione moiety of the L^n ligands are involved in the chelation. The L^n ligands are almost planar in the structure of **2** as measured by the angle of 2.01° (**2**) between planes H and P (see above; Table 4S†). However, they are considerably twisted in **4** and **5** with angles of 34.49 and 38.46°, respectively, involving those planes; in **3** that parameter assumes intermediate values (8.61 and 11.42°).

In all the structures the bond distances of 1.202(8)–1.308(4) Å for the N–N hydrazone groups suggest a double bond character.

Specific aspects of the structures. In complex **2** one $(H_2L^1)^{2-}$ anion, one water and one imidazole molecule fulfil a square pyramidal geometry ($\tau_5 = 0.02$)[8a] around the Cu^{II} cation, the hydrazone and the imidazole ligands occupying the equatorial positions and the water the axial site. This complex shows

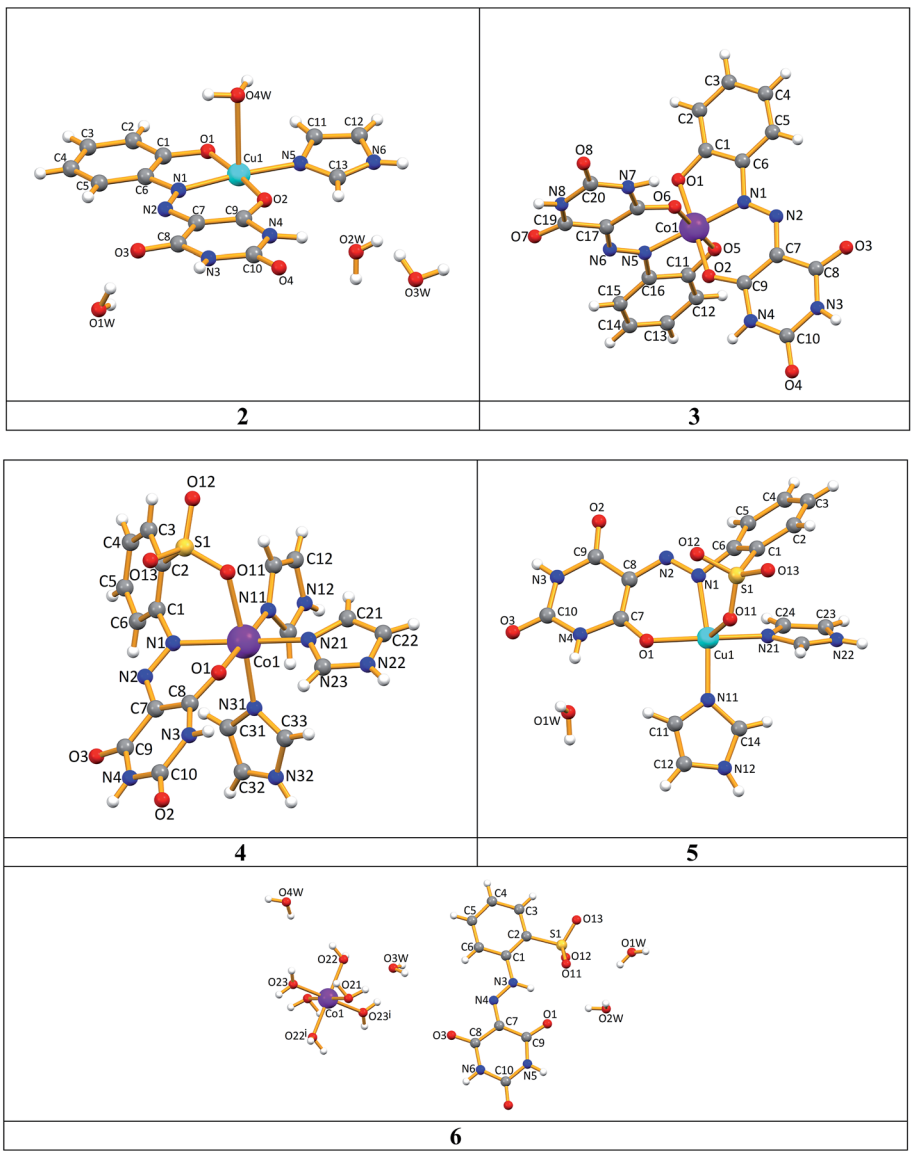

Fig. 1 X-ray molecular structures of **2–6** with atom numbering schemes. In **3** the hexaaquacobalt^{II} cation and the crystallization water molecules are omitted for clarity. Symmetry operations to generate equivalent atoms: (i) 1 − *x*, −*y*, −*z* (**6**).

a considerably elongated axial Cu–O_{water} length [2.545(4) Å] relative to the other metal–oxygen distances [1.921(4) and 1.925(4) Å] suggesting a tetragonal elongation, according to Addison's criteria,[8a] of av. 32% probably arising from different donor properties of the coordinated N- and O-atoms or from steric constrains from the ligands.

The structure of **3** comprises two Co^{III} (anionic part $\{[C_{20}H_{12}Co^{III}N_8O_8]^-\}_2$) and one Co^{II} (cationic part $[Co(H_2O)_6]^{2+}$) complex units, one of them involving two ONO chelating hydrazone $(H_2L^1)^{2-}$ anions and the other six coordinated water molecules (Scheme 2). For the anionic part of **3**, $[Co(H_2O)_6]^{2+}$ is counter ion rendering the compound neutral. Both metal centres show slightly distorted octahedral environments as expressed by the octahedral quadratic elongation (OQE) values of 1.002 and 1.001, and octahedral angle variations (OAV) of 6.03 and 1.47°[2], respectively.[8b] The hydrazone ligands in **3** are oriented in such a way that the two pairs of M–O bonds are mutually *trans*, as well as the pair of M–N bonds.

The Co^{II} coordination sphere in **4** comprises one $(H_2L^2)^{2-}$ anion and three imidazole ligands accomplishing a distorted octahedral environment around the cobalt cation (OQE and OAV of 1.008 and 25.55°[2], in this order). The Co–O bond lengths comprising the hydrazone derivative assume values of 2.104(5) and 2.195(4) Å and concern the O_{ketone} and $O_{sulfonyl}$, respectively; the Co–N distance, in turn, take a value of 2.118(5) Å. The Co–N distances concerning the imidazole ligands in **4** range from 2.110(5) to 2.134(6) Å, the longer one conceivably resulting from a *trans* effect of the coordinated sulfonyl O atom of the hydrazone ligand. The molecules of **4** are associated into infinite 1D chains along the crystallographic *b* axis by means of intermolecular N–H···O interactions involving one of the imidazole groups and one of the non-coordinated sulfonyl O-atoms (Fig. 10S and Table 4S†). The intermolecular metal···metal distance in **4** (8.608 Å) is considerably longer than that found in **3** (5.653 Å).

The Cu^{II} cation in **5** presents a square pyramidal geometry ($\tau_5 = 0.02$),[8] the equatorial plane being occupied by the O_{ketone}- and N-atoms from $(H_2L^2)^{2-}$, as well as two N-atoms from two imidazole ligands; the axial site is engaged with one of the $O_{sulfonyl}$ atoms from the hydrazone. As found in **2**, the coordination distance to the axial atom is longer than those to the equatorial atoms, although the tetragonal elongation[8a] is shorter (avg. 16%). The intermolecular metal···metal distance in **5** (6.603 Å) is slightly longer to that found in **2** (5.590 Å).

The structure of **6** also contains three-centred RAHB interactions[4,7d] in the anionic hydrazone units involving the O_{ketone}- and $O_{sulfonyl}$-atoms, which relates to the synergistic mutual reinforcement of intramolecular hydrogen bonding due to π-electron delocalization. The typical double bond lengths of $C_{pyrimidine}$–$N_{hydrazone}$ in the structure of **6** [1.314(3) Å] and the formation of the intramolecular N–H···O RAHB contacts indicate that hydrazone is the preferred tautomeric form in these cases.

The structures of this work contain trapped water molecules (except **4**) which interact among themselves and with the metal–organic (**2**, **3** and **5**) hosts *via* intermolecular hydrogen bonds. Such interactions, together with others involving the O- and N-atoms of pyrimidine trione rings as well as the coordinated water molecules (in **2**, **3** and **6**; Fig. 10S†), give rise to intricate 3D supramolecular frameworks.

Electrochemical behaviour of H_4L^1 and 1–6

In view of the application of **2–6** as homogeneous catalysts in oxidation processes in acetonitrile solution, the redox properties of H_4L^1 and **1–6** were studied by cyclic voltammetry (CV) and controlled potential electrolysis (CPE) at a platinum working electrode at 25 °C in a 0.2 M $[^nBu_4N][BF_4]$/NCMe solution. H_4L^1 and the Na^I complex **1** revealed to be redox active (Table 1, Fig. 11S and 12S†), exhibiting, by CV, an irreversible oxidation wave at $^IE_p^{ox}$ 1.2 V *vs.* SCE and an irreversible reduction wave ($^IE_p^{red}$) at *ca.* −0.9 to −1.1 V *vs.* SCE. Whereas the oxidation process appears not be affected by the nature or position of the substituents of the aromatic ring, the reduction one is more sensitive (a difference of 0.16 V *vs.* SCE is observed, Table 1). The redox processes at **1** are centred on the ligands. The copper^{II} complexes **2** and **5** exhibit, besides the redox processes centred on the ligands ($^IE_p^{ox}$ and $^IE_p^{red}$, Table 1), a two-electrons (as measured by CPE) irreversible cathodic wave at $^{II}E_p^{red}$ −1.56 V or −1.67 *vs.* SCE, respectively, assigned to the $Cu^{II} \rightarrow Cu^0$ reduction (Fig. 13S†).[9a,b] The CPE performed at these potentials lead to the deposition of metallic copper which is clearly detected by its sharp oxidation (with desorption) wave at $E_p^{ox} = -0.09$ (**2**) (Fig. 13S†) or −0.11 (**5**) V *vs.* SCE. For the Co complexes **3**, **4** and **6**, the irreversible oxidation waves ($^IE_p^{ox}$ and $^{II}E_p^{ox}$, Table 1) are conceivably centred on the organic ligands, as well as the irreversible reduction waves in the range of −0.8 to −1.0 V *vs.* SCE. However, in **3**, the extra reversible reduction wave at $^IE_{1/2}^{red} = -0.21$ V is assigned to the $Co^{III} \rightarrow Co^{II}$ reduction of the $[Co^{III}(H_2L^1)_2]^-$ anionic complex part (see Fig. 14S†). Those potentials are much lower than that ($^IE_p^{ox} = 1.63$ V, Table 1) observed for the $Co^{II} \rightarrow Co^{III}$ oxidation in the salt $Co(NO_3)_2$ salt and also in mononuclear Co complexes bearing C-scorpionate[9c] or pyrazole[9d] ligands (1.03 to 1.52 V *vs.* SCE).[9d]

Table 1 Cyclic voltammetric data[a] for compounds H_4L^1 and **1–6**

Compound	$^IE_p^{ox}$	$^{II}E_p^{ox}$	$^IE_p^{red}$ ($^IE_{1/2}$)	$^{II}E_p^{red}$
H_4L^1	1.22	—	−0.93	—
1	1.21	—	−1.09	—
2[b]	0.78	—	−0.82	−1.56
3	0.92	1.08	(−0.21)	−0.83
4	0.82	1.13	−1.14	—
5[c]	1.04	—	−1.16	−1.67
6	1.11	1.19	−1.02	—
$Co(NO_3)_2 \cdot 6H_2O$[d]	1.63	—	—	—

[a] Potential values in volt ± 0.02 *vs.* SCE, in a 0.2 M $[Bu_4N][BF_4]$/NCMe solution, at a Pt disc working electrode determined by using the $[Fe(\eta^5\text{-}C_5H_5)_2]^{0/+}$ redox couple ($E_{1/2}^{ox} = 0.42$ V *vs.* SCE[10]) as internal standard at a scan rate of 200 mV s^{-1}. [b] An anodic (with desorption) wave at $E_p^{ox} = -0.09$ V is generated upon scan reversal following the second reduction wave. [c] An anodic (with desorption) wave at $E_p^{ox} = -0.11$ V is generated upon scan reversal following the second reduction wave. [d] For comparison purposes.

Catalytic activity of metal complexes for cyclohexane oxidation

Compounds **1–6** and the proligand $\mathbf{H_4L^1}$ were tested as catalysts for the peroxidative (with aqueous hydrogen peroxide) oxidation, at room temperature, of cyclohexane (CyH) to the mixture of cyclohexyl hydroperoxide (CyOOH, primary product) with cyclohexanol (CyOH) and cyclohexanone (Cy_{-H}=O) (final products) (Scheme 4). As expected, the non-metallic species $\mathbf{H_4L^1}$, as well as the sodium compound **1**, were not able to catalyse the above reaction in the tested conditions. The compounds **2–6** act as catalyst precursors for such an oxidation, **2** and **3** being the most active ones (Table 2). Thus, **2** and **3**, derived from *ortho*-OH AHBA ligand, show high activity in comparison to other complexes from its *ortho*-SO_3H substituted version. The catalytic activity of Co^{II} complexes (**4** and **6**) is higher than of Cu^{II} one (**5**) derived from same *ortho*-SO_3H substituted ligand, $\mathbf{H_4L^2}$. Nevertheless, the catalytic performances of **4** and **6** are different (11 and 8% correspondingly, entries 5 and 9). Such differences possibly reflect the different coordination environment of Co^{II} and labilities of the coordinated imidazole and water ligands in those complexes. The easy reduction of the Cu^{II} complex **2** detected by cyclic voltammetry (Table 1) can also have a favourable effect on its catalytic activity.

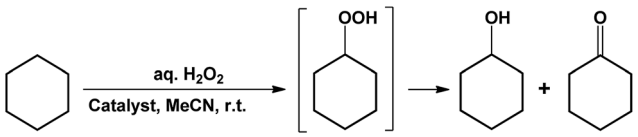

Scheme 4 Oxidation of cyclohexane catalysed by **2–6**.

In fact, after 6 h stirring the reaction mixture (CyH, H_2O_2 30% aq. and the copper or cobalt catalyst **2** or **3**, respectively, in MeCN) at room temperature, a 21% overall yield (relative to the cyclohexane) of cyclohexanol and cyclohexanone was obtained with an overall turnover number (TON) of 213 (**3**) (71 per Co atom) or 10 (**2**) moles of products per mole of catalyst precursor (entries 3 and 19, respectively, Table 2).

The formation of CyOOH (under the conditions of Table 2) is proved by using the method proposed by Shul'pin.[6d,10] The addition of PPh_3 prior to the GC analysis of the products results in a marked increase of the amount of cyclohexanol (compare entries 1 and 11, Table 2) due to reduction of CyOOH by PPh_3, with formation of phosphane oxide, and a corresponding decrease of cyclohexanone, as observed in other catalytic systems.[11]

Table 2 Peroxidative oxidation of cyclohexane[a] with H_2O_2 (selected data) catalysed by **2–6**

Entry	Catalyst	n(Cat)/n(CyH) × 10^3	$n(H_2O_2)/n$(Cat) × 10^{-3}	Yield (%)[b] CyOH	Cy_{-H}=O	total[e]	TON[c]	CyOH/Cy_{-H}=O ratio	Select.[d] (%)
1	**2**	1	2	15.7	0.5	16.2	162	31.4	98
2[f]	**2**	1	2	0.1	0.1	0.2	2	1.0	96
3	**3**	1	2	20.4	0.9	21.3	213	22.7	96
4[f]	**3**	1	2	2.8	0.7	3.5	35	4.0	89
5	**4**	1	2	5.2	5.3	10.5	105	1.0	91
6[f]	**4**	1	2	1.7	0.1	1.8	18	17.0	94
7	**5**	1	2	2.9	2.7	5.6	56	1.1	89
8[f]	**5**	1	2	1.9	0.3	2.2	22	6.3	94
9	**6**	1	2	5.5	2.6	8.1	81	2.1	98
10[f]	**6**	1	2	0.2	0	0.2	2	—	93
11[g]	**2**	1	2	5.3	9.4	14.7	147	0.6	64
12	**2**	1	0.1	1.1	1.2	2.3	23	0.9	89
13	**2**	1	0.2	5.4	2.9	8.3	83	1.9	91
14	**2**	1	1	8.6	5.3	13.9	139	1.6	89
15	**2**	1	10	4.2	2.7	6.9	69	1.6	41
16	**2**	0.2	2	3.1	2.1	5.2	260	1.5	93
17	**2**	3	2	12.2	6.7	18.9	63	1.8	88
18	**2**	10	2	11.7	8.3	20.0	20	1.4	84
19	**2**	20	2	18.1	2.5	20.6	10	7.2	83
20[h]	**2**	1	2	0.8	0.6	1.4	14	1.3	39
21[i]	**2**	1	2	1.9	1.2	3.1	31	1.6	56
22[j]	**2**	1	2	11.2	4.6	15.8	158	2.4	99
23	$Cu(NO_3)_2$	1	2	2.9	1.2	4.1	41	2.4	39
24	$Co(NO_3)_2$	1	2	4.7	2.6	7.3	73	1.8	61
25	$[Cu(im)_4](NO_3)_2$	1	2	4.3	3.3	7.6	76	1.3	73
26	$[Co(im)_6](NO_3)_2$	1	2	5.2	3.9	9.1	81	1.3	84

[a] Reaction conditions (unless stated otherwise): MeCN (3 mL), cyclohexane (5.0 mmol), 0.5–20 μmol of **2–6**, H_2O_2 (10.0 mmol), 6 h, r.t.; yield and TON determined by GC analysis (upon treatment with PPh_3). [b] Molar yield (%) based on substrate, *i.e.* moles of products (cyclohexanol (CyOH) and cyclohexanone (Cy_{-H}=O)) per 100 mol of cyclohexane. [c] Turnover number (moles of product per mol of catalyst precursor). [d] Selectivity (moles of cyclohexanol and cyclohexanone per mole of converted substrate). [e] Moles of cyclohexanol + cyclohexanone per 100 moles of cyclohexane. [f] Reaction in the presence of HNO_3 [$n(HNO_3)/n$(catalyst) = 30]. [g] Without addition of PPh_3. [h] Reaction in the presence of $CBrCl_3$ (5.0 mmol). [i] Reaction in the presence of Ph_2NH (5.0 mmol). [j] Reaction performed under nitrogen atmosphere.

The selectivity towards the cyclohexanol + cyclohexanone mixture is rather high, even for the high yields (*e.g.* 96% selectivity for 21% yield, entry 3, Table 2). This is much better than what obtained in the current industrial process (*ca.* 4% yield for *ca.* 85% selectivity),[6a,h,12] in spite of the mild reaction conditions used in our case. Our yields are similar to reported for dinuclear Cu^{II} complexes[11a] (22–29%) or scorpionate Cu^{II} (ref. 11*c*) or Co^{III},[9c,11f] complexes (up to 23%). As can be seen in Table 2, $Cu(NO_3)_2$, $Co(NO_3)$, $[Cu(im)_4](NO_3)_2$ and $[Co(im)_6](NO_3)_2$ provide only 4, 7, 8 and 9% total yield (entries 23–26), respectively. The high catalytic activity of **3** is expected to be due to its anionic part $[C_{20}H_{12}Co^{III}N_8O_8]^-$ since the cationic part $[Co(H_2O)_6]^{2+}$ can also be derived from $Co(NO_3)_2$ in solution, which provides low yield (entry 24, Table 2).

The catalytic performance of **2** and **3** under the same conditions, but replacing the oxidant by dioxygen, was assessed. It was found a negligible conversion of cyclohexane into the oxygenated products, thus suggesting the need of a peroxide oxidant, such as hydrogen peroxide, for this mild oxidative process.

The previously recognized common promoting effect of an acidic medium[11d,f,13] on the peroxidative oxidation of alkanes is not observed for the present systems (Table 2). On the contrary, the presence of nitric acid has a drastic inhibiting effect on the catalytic activity of all the compounds tested (Fig. 2). Due to formation, in acidic medium, of stable a RAHB system in ligand molecules, complexes are not stable, *i.e.*, protonation of ligands breaks down the active species (complex molecules) and therefore catalytic activity decreases. A similar behaviour was found for Cu^{II} complexes bearing azathia macrocycles[14] and also for C-scorpionate Au^{III} complexes.[15]

The effect of the peroxide to catalyst molar ratio was also investigated (entries 1, 12–15, Table 2) and is depicted in Fig. 3. The increase of the peroxide amount up to $n(H_2O_2)/n$(catalyst) molar ratio of 2×10^3 leads to the maximum product yield and TON (Table 2, entry 1, Fig. 4). Further increase of the oxidant amount (up to 1×10^4) results in a strong yield drop (entry 15) eventually due to overoxidation reactions. In fact, for this oxidant to catalyst molar ratio, 1,4-cyclohexanedione was detected by CG-MS as the main overoxidation product (3.2% relative to cyclohexane). 1,3-Cyclohexanediol, 1,4-cyclohexanediol, 1,4-hydroxycyclohexanone, and 1,2-epoxycyclohexane were also detected, but in much lower amounts (1.4, 1.1, 0.3 and 0.2%, respectively, relative to cyclohexane).

The activities of our catalytic systems are also dependent on the reaction time. Yields tend to increase on the extension of reaction time from up to 6 h (Fig. 5) whereafter a further increase of reaction time results in a yield drop due to subsequent reactions. In fact, overoxidation products such as 1,3-cyclohexanediol, 1,4-cyclohexanediol, 1,4-hydroxycyclohexanone, 1,4-cyclohexanedione or 1,2-epoxycyclohexane (*e.g.*, 1.1, 0.8, 0.5, 0.9 or 0.3%, respectively, relative to cyclohexane, for **3**) were detected by CG-MS for 9 h reaction time.

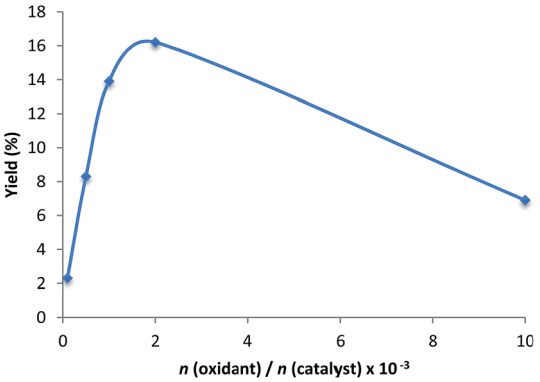

Fig. 3 Effect of the molar H_2O_2 to catalyst ratio on the overall yield (cyclohexanol + cyclohexanone) using **2** as catalyst precursor.

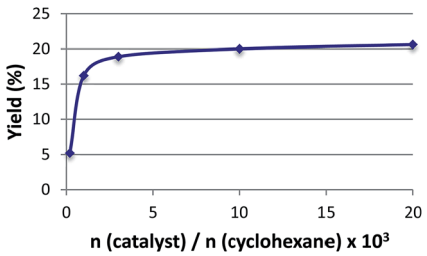

Fig. 4 Effect of the molar catalyst to cyclohexane ratio on the overall yield (cyclohexanol + cyclohexanone) using **2** as catalyst.

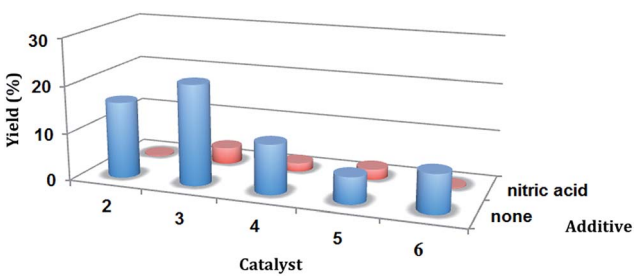

Fig. 2 Catalytic activity of **2–6** for the oxidation of cyclohexane. Effect of the presence of nitric acid on the overall yield (cyclohexanol + cyclohexanone) using **2–6** as catalysts.

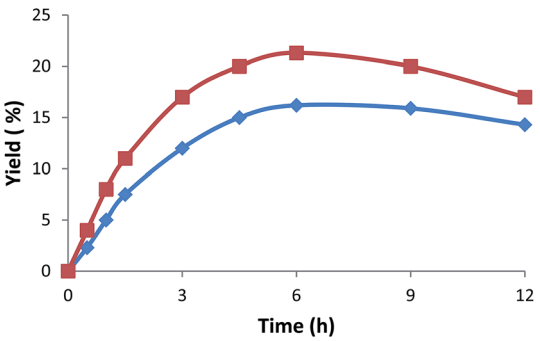

Fig. 5 Dependence of the overall yield (mol%, based on substrate) of the products on the reaction time. Reaction conditions: MeCN (3.0 mL), cyclohexane (5.0 mmol), 5 μmol of **2** or **3** $n(H_2O_2)/n$(catalyst precursor) (2×10^3), r.t.

A noteworthy feature of the studied oxidations is the use of low catalyst loadings (typically 0.1 mol% *vs.* substrate) with high yields of oxygenated products (Table 2) considering the inertness of the substrate.

As observed for several metal catalytic systems,[11,13,14] addition of a radical trap ($CBrCl_3$ or Ph_2NH) to the reaction mixture (Table 2, entries 20 and 21, respectively) results in a considerable suppression of the catalytic activity. This behaviour, along with the formation of cyclohexyl hydroperoxide (CyOOH, typical intermediate product in radical-type reactions) suggests a free-radical mechanism for cyclohexane oxidation, which will be further investigated.

Conclusions

In this study we have successfully used AHBA chelating ligands bearing barbituric acid fragment, as well as –OH and $-SO_3H$ groups in *ortho*-position of the aromatic part, and in several cases, imidazole (as an auxiliary ligand or a deprotonating agent for the weakening/destroying RAHB system in AHBA), to synthesis novel mononuclear Co^{II}, $Co^{II/III}$ and Cu^{II} complexes. AHBA ligands play a crucial structural role in the organization of the H-bonded assemblies, influencing the overall 3D supramolecular arrangement (also depending on the metal ions) and imparting water solubility to the complexes.

The Cu^{II} and $Co^{II/III}$ derivatives **2** and **3**, respectively, display a high catalytic activity for the peroxidative (with H_2O_2) oxidation of cyclohexane in aqueous acetonitrile medium, under mild conditions.

Experimental

Materials and instrumentation

The ^1H and ^{13}C NMR spectra were recorded at room temperature on a Bruker Avance II + 300 (UltraShield™ Magnet) spectrometer operating at 300.130 and 75.468 MHz for proton and carbon-13, respectively. The chemical shifts are reported in ppm using tetramethylsilane as the internal reference. The infrared spectra (4000–400 cm^{-1}) were recorded on a BIO-RAD FTS 3000MX instrument in KBr pellets. Carbon, hydrogen, and nitrogen elemental analyses were carried out by the Microanalytical Service of the Instituto Superior Técnico. Electrospray mass spectra (ESI-MS) were run with an ion-trap instrument (Varian 500 MS LC Ion Trap Mass Spectrometer) equipped with an electrospray ion source. For electrospray ionization, the drying gas and flow rate were optimized according to the particular sample with 35 p.s.i. nebulizer pressure. Scanning was performed from m/z 100 to 1200 in methanol solution. The compounds were observed in the negative or positive mode (capillary voltage = 80–105 V). The UV-vis absorption spectra in the 200–700 nm region were recorded with a scan rate of 240 nm min^{-1} by using a Lambda 35 UV-vis spectrophotometer (Perkin-Elmer) in 1.00 cm quartz cells at room temperature, with a concentration of $\mathbf{H_4L^1}$ and **1–6** of 2.00×10^{-5} M in water. Chromatographic analyses were undertaken by using a Fisons Instruments GC 8000 series gas chromatograph with a DB-624 (J&W) capillary column (FID detector) and the Jasco-Borwin v.1.50 software. The internal standard method was used to quantify the organic products. The electrochemical experiments were performed on an EG&G PAR 273A potentiostat/galvanostat connected to a personal computer through a GPIB interface. Cyclic voltammetry (CV) studies were undertaken in 0.2 M $[^nBu_4N][BF_4]$/MeCN, at a platinum disc working electrode ($d = 0.5$ mm) and at room temperature. Controlled-potential electrolyses (CPE) were carried out in electrolyte solutions with the above-mentioned composition, in a three-electrode H-type cell. The compartments were separated by a sintered glass frit and equipped with platinum gauze working and counter electrodes. For both CV and CPE experiments, a Luggin capillary connected to a silver wire pseudo-reference electrode was used to control the working electrode potential. A Pt wire was employed as the counter-electrode for the CV cell. The CPE experiments were monitored regularly by CV thus assuring no significant potential drift occurred along the electrolysis. The solutions were saturated with N_2 by bubbling this gas before each run, the redox potentials of the complexes were measured by CV in the presence of ferrocene as the internal standard, and their values are quoted relative to the SCE by using the $[Fe(\eta^5\text{-}C_5H_5)_2]^{0/+}$ redox couple ($E^{ox}_{1/2} = 0.42$ V *vs.* SCE).[9]

Syntheses of H_4L^1 and 1

The arylhydrazones of barbituric acid, 5-(2-(2-hydroxyphenyl)-hydrazono)pyrimidine-2,4,6(1*H*,3*H*,5*H*)-trione ($\mathbf{H_4L^1}$) and sodium salt of 2-(2-(2,4,6-trioxotetrahydropyrimidin-5(2*H*)-ylidene)hydrazinyl) benzenesulfonic acid ($\mathbf{H_4L^2}$), $[Na(H_3L^2)(\mu\text{-}H_2O)(H_2O)_2]_2$ (**1**), were synthesized according to the Japp–Klingemann reaction[2,7] between the aromatic diazonium salt of substituted aniline and barbituric acid.

Diazotization. 2-substituted aniline (20 mmol) was dissolved in 50 mL water, and 0.40 g (10 mmol) of NaOH was added. The solution was cooled in an ice bath to 273 K and 1.38 g (20 mmol) of $NaNO_2$ were added; 4.00 mL HCl were then added in 0.5 mL portions for 1 h. The temperature of the mixture should not exceed 278 K.

Azocoupling. NaOH (0.80 g, 20 mmol) was added to a mixture of 20 mmol (2.56 g) of barbituric acid with 50.00 mL of water. The solution was cooled in an ice bath, and a suspension of 2-substituted aniline diazonium (prepared according to the procedure described above) was added in two equal portions under vigorous stirring for 1 h. The formed precipitate of the ligand was filtered off, recrystallized from methanol and dried in air. The characterizations of the ligands were carried out by IR, ^1H and ^{13}C-NMR spectroscopies and are given below.

H_4L^1. Yield, 3.72 g, 75% (based on barbituric acid), orange powder soluble in DMSO, DMF, water, methanol, acetone and acetonitrile. Anal. calcd for $C_{10}H_8N_4O_4$ ($Mr = 248.05$): C, 48.39; H, 3.25; N, 22.57; found: C, 48.07; H, 3.11; N, 22.32%. ESI-MS: m/z: 249.2 $[Mr + H]^+$. IR (KBr): 3453 ν(OH), 3041, 2844 and 2736 ν(NH), 1731 and 1697 ν(C=O), 1643 ν(C=O···H), 1597 ν(C=N) cm^{-1}. ^1H NMR (300.130 MHz) in DMSO-d_6, internal TMS, δ (ppm): 6.94–7.60 (4H, Ar–H), 10.62 (s, 1H, O–H), 11.23 (s, 1H, N–H), 11.44 (s, 1H, N–H), 14.44 (s, 1H, N–H). $^{13}C\{^1H\}$ NMR

(75.468 MHz, DMSO-d_6). δ: 115.10, 115.94, 117.79 and 120.09 (Ar–H), 126.82 (Ar–NHN =), 129.09 (C=N), 146.63 (Ar–OH), 149.86 and 160.01 (C=O), 162.50 (C=O···H).

1. Yield, 4.42 g, 57% (based on barbituric acid), light orange powder soluble in DMSO, DMF, water, methanol, acetone and acetonitrile. Anal. calcd for $C_{20}H_{26}N_8Na_2O_{18}S_2$ (Mr = 776.06): C, 30.93; H, 3.37; N, 14.43; found: C, 30.76; H, 3.23; N, 14.24%. ESI-MS: m/z: 702.1 $[Mr - 4H_2O + H]^+$. IR (KBr): 3452 ν(OH), 3065 and 2964 ν(NH), 1739 and 1677 ν(C=O), 1604 ν(C=O···H), 1520 ν(C=N) cm^{-1}. ^1H NMR (300.130 MHz) in DMSO-d_6, internal TMS, δ (ppm): 7.21–7.80 (4H, Ar–H), 11.24 (s, 1H, N–H), 11.35 (s, 1H, N–H), 14.80 (s, 1H, N–H). $^{13}C\{^1H\}$ NMR (75.468 MHz, DMSO-d_6). δ: 116.21, 118.25, 125.01 and 127.59 (Ar–H), 130.53 (Ar–NHNC=), 135.86 (C=N), 138.17 (Ar–SO_3Na), 150.11 and 160.32 (C=O), 160.74 (C=O···H). The crystals of **1** suitable for X-ray structural analysis were obtained by slow evaporation of a methanol solution of the light orange powder.

Syntheses of 2–6

Synthesis of 2. 248 mg (1 mmol) of $\mathbf{H_4L^1}$ were dissolved in water–acetone mixture (1 : 4, v/v), then 136 mg (2 mmol) of imidazole (im) were added, under stirring. The addition of 232 mg (1 mmol) of $Cu(NO_3)_2 \cdot 2.5H_2O$ together with 10 mL of distilled water resulted in a clear solution. The resulting solution was allowed to stand at room temperature and brown crystals of **2** were obtained after 1 day.

2: Yield, 229 mg, 51% (based on $\mathbf{H_4L^1}$). It is soluble in water, DMSO, methanol, DMF, acetone and acetonitrile. Anal. calcd for $C_{13}H_{18}CuN_6O_8$ (Mr = 449.86): C, 34.71; H, 4.03; N, 18.68%. Found: C, 34.45; H, 3.95; N, 18.44%. IR (KBr): 3424 (s br) ν(H_2O), 3060, 2870 and 2740 ν(NH), 1714 ν(C=O), 1586 ν(C=N) cm^{-1}. ESI-MS: m/z: 310.7 $[C_{10}H_6CuN_4O_4 + H]^+$.

Synthesis of 3. 248 mg (1 mmol) of $\mathbf{H_4L^1}$ were dissolved in water–acetone mixture (1 : 4, v/v), then 200 μL of triethylamine (Et_3N) and 291 mg (1 mmol) of $Co(NO_3)_2 \cdot 6H_2O$ were added at room temperature. The mixture was stirred for 30 min and left standing for slow solvent evaporation. Red crystals of **3** suitable for X-rays started to form in the reaction mixture after 1 day at room temperature; after 2 d they were filtered off and dried in air.

3: Yield, 282 mg, 60% (based on Co). It is soluble in water, DMSO, methanol, DMF, acetonitrile and acetone. Anal. calcd for $C_{40}H_{52}Co_3N_{16}O_{30}$ (Mr = 1413.73): C, 33.98; H, 3.71; N, 15.85%. Found: C, 33.66; H, 3.80; N, 15.67%. IR (KBr): 3451 (s br) ν(H_2O), 3073, 2875 and 2733 ν(NH), 1719 ν(C=O), 1594 ν(C=N) cm^{-1}. ESI-MS: m/z: 167.0 $[Co(H_2O)_6]^{2+}$ and 551.2 $[C_{20}H_{12}CoN_8O_8]^-$.

Syntheses of 4 and 5. 776 mg (1.0 mmol) of **1** was dissolved in 15 mL water–acetone mixture (1 : 4, v/v), then 291 mg (1.0 mmol) of $Co(NO_3)_2 \cdot 6H_2O$ (232 mg of $Cu(NO_3)_2 \cdot 2.5H_2O$ in the case of **5**) and 204 mg (3.0 mmol) im (136 mg im in the case of **5**) were added. The mixture was stirred for 5 min at 80 °C, then left for slow evaporation. Black (green in the case of **5**) crystals of the product started to form after *ca.* 2 d at room temperature; they were then filtered off and dried in air.

4: Yield, 298 mg, 52% (based on Co). It is soluble in water, DMSO, methanol and DMF. Anal. calcd for $C_{19}H_{18}CoN_{10}O_6S$ (Mr = 573.41): C, 39.80; H, 3.16; N, 24.43%. Found: C, 39.74; H, 3.05; N, 24.32%. IR (KBr): 3380, 3220 and 2801 ν(NH), 1738 and 1664 ν(C=O), 1589 ν(C=N) cm^{-1}. ESI-MS: m/z: 574.0 $[Mr + H]^+$.

5: Yield, 290 mg, 55% (based on Cu). It is soluble in water, DMSO, methanol and DMF. Anal. calcd for $C_{16}H_{16}CuN_8O_7S$ (Mr = 527.96): C, 36.40; H, 3.05; N, 21.22%. Found: C, 36.14; H, 3.00; N, 21.14%. IR (KBr): 3454 ν(OH), 3145, 3075, 2980, 2892 and 2797 ν(NH), 1720, 1633 and 1606 ν(C=O), 1521 ν(C=N) cm^{-1}. ESI-MS: m/z: 510.0 $[Mr - H_2O + H]^+$.

Synthesis of 6. 776 mg (1 mmol) of **1** was dissolved in water–acetone mixture (1 : 4, v/v), then 200 μL of triethylamine (Et_3N) and 291 mg (1 mmol) of $Co(NO_3)_2 \cdot 6H_2O$ were added and the system heated to 80 °C for 10 min and left for slow evaporation. Red crystals of **7** started to form after *ca.* 2 d at room temperature; they were then filtered off and dried in air.

7: Yield, 229 mg, 49% (based on Co). It is soluble in water, DMSO, methanol, DMF, acetonitrile and acetone. Anal. calcd for $C_{20}H_{42}CoN_8O_{26}S_2$ (Mr = 933.65): C, 25.73; H, 4.53; N, 12.00%. Found: C, 25.75; H, 4.42; N, 11.95%. IR (KBr): 3455 ν(OH), 3064, 2872 and 2677 ν(NH), 1738, 1675 and 1580 ν(C=O), 1520 ν(C=N) cm^{-1}. ESI-MS: m/z: 312.1 $[H_3L^3 + H]^+$ and 682.1 $[Co(H_3L^3)_2 + H]^+$.

X-ray structure determinations

X-ray quality single crystals of the compounds were mounted in a nylon loop and measured at 150 K (**1** and **3**) or at room temperature (**2** and **4–6**). Intensity data were collected using a Bruker AXS-KAPPA APEX II diffractometer or a Bruker APEX-II PHOTON 100 diffractometer with graphite monochromated Mo-Kα (λ 0.71069) radiation. Data were collected using phi and omega scans of 0.5° per frame and a full sphere of data was obtained. Cell parameters were retrieved using Bruker SMART[16a] software and refined using Bruker SAINT[16a] on all the observed reflections. Absorption corrections were applied using SADABS.[16a] Structures were solved by direct methods by using the SHELXS package[16b] and refined with SHELXL-2014.[16b] Calculations were performed using the WinGX System-Version 1.80.03.[16c] The hydrogen atoms of water, hydrazine or ammonium groups were found in the difference Fourier map and the isotropic thermal parameters were set at 1.5 times the average thermal parameters of the belonging oxygen or nitrogen atoms, frequently with their distances restrained by using the DFIX and DANG commands. Coordinates of hydrogen atoms bonded to carbon atoms were included in the refinement using the riding-model approximation with the Uiso(H) defined as 1.2Ueq of the parent aromatic or methylene atoms. There were disordered molecules present in the structure of **4**. Since no obvious major site occupations were found for those molecules, it was not possible to model them. PLATON/SQUEEZE[16d] was used to correct the data. A total of 136 electrons were estimated but the assignment is dubious. Thus, they were simply removed from the model. Least square refinements with anisotropic thermal motion parameters for all the non-hydrogen atoms and isotropic ones for the remaining atoms were employed. ESI.†

Oxidation of cyclohexane

Typical reaction mixtures were prepared as follows: to 0.5–20.0 μmol of the compound $\mathbf{H_4L^1}$ and **1–6** contained in the reaction flask were added 3 mL of MeCN, 5.00 mmol of C_6H_{12} and 10 mmol of H_2O_2 solution (30% in H_2O). In the experiments with radical traps, $CBrCl_3$ (5.00 mmol) or $NHPh_2$ (5.00 mmol) was added to the reaction mixture. The reaction mixture was stirred for 6 h at room temperature (*ca.* 298 K) and air atmospheric pressure, then 90 μL of cycloheptanone (as internal standard) and 5.0 mL of diethyl ether (to extract the substrate and the products from the reaction mixture) were added. The resulting mixture was stirred for 15 min and then a sample taken from the organic phase was analysed by GC. Subsequently, PPh_3 was added to the final organic phase (to reduce the cyclohexyl hydroperoxide), the mixture was analysed again to estimate the amount of cyclohexyl hydroperoxide, according to Shul'pin's method.[10] Blank experiments were performed and confirmed that no cyclohexane oxidation products were obtained in the absence of the metal catalyst precursor.

Acknowledgements

This work has been partially supported by the Foundation for Science and Technology (FCT), Portugal (UID/QUI/00100/2013 program). The authors acknowledge the Portuguese NMR Network (IST-UTL Centre) for access to the NMR facility, and the IST Node of the Portuguese Network of mass-spectrometry (Dr Conceição Oliveira) for the ESI-MS measurements. The authors also acknowledge the financial support by the University of Camerino (Fondo di Ateneo per la Ricerca 2011–2012) and Nuova Simonelli Company.

References

1 (*a*) A. Slaczka and J. Lubczak, *J. Appl. Polym. Sci.*, 2007, **106**, 4067–4074; (*b*) D. Thetford, A. P. Chorlton and J. Hardman, *Dyes Pigm.*, 2003, **59**, 185–191; (*c*) M. R. Zamanloo, A. Shamkhali, M. Alizadeh, Y. Mansoori and G. Imanzadeh, *Dyes Pigm.*, 2012, **95**, 587–599; (*d*) M. Tishler, K. Pfister, R. D. Babson, K. Ladenburg and A. J. Fleming, *J. Am. Chem. Soc.*, 1947, **69**, 1487–1492.

2 K. T. Mahmudov, M. N. Kopylovich, A. M. Maharramov, M. M. Kurbanova, A. V. Gurbanov and A. J. L. Pombeiro, *Coord. Chem. Rev.*, 2014, **265**, 1–37.

3 (*a*) E. Colacio, J. Ruiz, J. M. Moreno, R. Kivekas, M. R. Sundberg, J. M. Dominguez-Vera and J. P. Laurent, *J. Chem. Soc., Dalton Trans.*, 1993, 157–163; (*b*) E. Colacio, M. Quiros, J. M. Salas, A. Garca and J. D. Martin, *J. Crystallogr. Spectrosc. Res.*, 1993, **23**, 407–410; (*c*) E. Colacio, J.-M. Dominguez-Vera, R. Kivekas and J. Ruiz, *Inorg. Chim. Acta*, 1994, **218**, 109–119; (*d*) E. Colacio, J.-M. Dominguez-Vera, J.-P. Costes, R. Kivekas, J.-P. Laurent, J. Ruiz and M. Sundberg, *Inorg. Chem.*, 1992, **31**, 774–778; (*e*) E. Colacio, J.-M. Dominguez-Vera, R. Kivekas, J. M. Moreno and J. Ruiz, *Inorg. Chim. Acta*, 1994, **219**, 127–133; (*f*) J. M. Moreno, J. Ruiz, J.-M. Dominguez-Vera, E. Colacio, D. Galisteo and R. Kivekas, *Polyhedron*, 1994, **13**, 203–207; (*g*) V. Sadasivan and M. Alaudeen, *Indian J. Chem., Sect. A: Inorg., Bio-inorg., Phys., Theor. Anal. Chem.*, 2007, **46**, 1959–1964; (*h*) K. T. Mahmudov, M. F. C. Guedes da Silva, M. Glucini, M. Renzi, K. C. P. Gabriel, M. N. Kopylovich, M. Sutradhar, F. Marchetti, C. Pettinari, S. Zamponi and A. J. L. Pombeiro, *Inorg. Chem. Commun.*, 2012, **22**, 187–189.

4 (*a*) M. N. Kopylovich, A. C. C. Nunes, K. T. Mahmudov, M. Haukka, T. C. O. Mac Leod, L. M. D. R. S. Martins, M. L. Kuznetsov and A. J. L. Pombeiro, *Dalton Trans.*, 2011, **40**, 2822–2836; (*b*) M. N. Kopylovich, K. T. Mahmudov, M. F. C. G. Silva, L. M. D. R. S. Martins, M. L. Kuznetsov, T. F. S. Silva, J. J. R. Fraústo da Silva and A. J. L. Pombeiro, *J. Phys. Org. Chem.*, 2011, **24**, 764–773; (*c*) M. N. Kopylovich, M. F. C. Guedes da Silva, L. M. D. R. S. Martins, M. L. Kuznetsov, K. T. Mahmudov and A. J. L. Pombeiro, *Polyhedron*, 2013, **50**, 374–382.

5 A. Mizar, M. F. C. Guedes da Silva, M. N. Kopylovich, S. Mukherjee, K. T. Mahmudov and A. J. L. Pombeiro, *Eur. J. Inorg. Chem.*, 2012, 2305–2313.

6 (*a*) *Ullmann's Encyclopedia of Industrial Chemistry*, Wiley-VCH, Weinheim, 6th edn, 2002; (*b*) G. B. Shul'pin, Oxidations of C–H Compounds Catalyzed by Metal Complexes, in *Transition Metals for Organic Synthesis*, ed. M. Beller and C. Bolm, Wiley–VCH, Weinheim, New York, 2nd edn, 2004, vol. 2, pp. 215−242; (*c*) G. B. Shul'pin, *Org. Biomol. Chem.*, 2010, **8**, 4217–4228; (*d*) G. B. Shul'pin, *Dalton Trans.*, 2013, **42**, 12794–12818; (*e*) A. E. Shilov and G. B. Shul'pin, *Activation and Catalytic Reactions of Saturated Hydrocarbons in the Presence of Metal Complexes*, Kluwer Academic Publishers, Dordrecht, The Netherlands, 2000; (*f*) M. N. Kopylovich, T. C. O. Mac Leod, M. Haukka, G. I. Amanullayeva, K. T. Mahmudov and A. J. L. Pombeiro, *J. Inorg. Biochem.*, 2012, **115**, 72–77; (*g*) M. N. Kopylovich, M. J. Gajewska, K. T. Mahmudov, M. F. C. Guedes da Silva, M. V. Kirillova, P. J. Figiel, J. Sanchiz and A. J. L. Pombeiro, *New J. Chem.*, 2012, **36**, 1646–1654; (*h*) U. Schuchardt, D. Cardoso, R. Sercheli, R. Pereira, R. S. da Cruz, M. C. Guerreiro, D. Mandelli, E. V. Spinacé and E. L. Pires, *Appl. Catal., A*, 2001, **211**, 1–17; (*i*) M. Sutradhar, N. V. Shvydkiy, M. F. C. Guedes da Silva, M. V. Kirillova, Y. N. Kozlov, A. J. L. Pombeiro and G. B. Shul'pin, *Dalton Trans.*, 2013, **42**, 11791–11803; (*j*) M. Sutradhar, L. M. D. R. S. Martins, M. F. C. Guedes da Silva and A. J. L. Pombeiro, *Coord. Chem. Rev.*, 2015, **301–302**, 200–239; (*k*) K. M. Parida, M. Sahoo and S. Singha, *J. Mol. Catal. A: Chem.*, 2010, **329**, 7–12.

7 (*a*) A. M. Maharramov, R. A. Aliyeva, I. A. Aliyev, F. G. Pashaev, A. G. Gasanov, S. I. Azimova, R. K. Askerov, A. V. Kurbanov and K. T. Mahmudov, *Dyes Pigm.*, 2010, **85**, 1–6; (*b*) K. T. Mahmudov, A. M. Maharramov, R. A. Aliyeva, I. A. Aliyev, R. K. Askerov, R. Batmaz, M. N. Kopylovich and A. J. L. Pombeiro, *J. Photochem. Photobiol., A*, 2011, **219**, 159–165; (*c*) S. R. Gadjieva, T. M. Mursalov, K. T. Mahmudov and F. M. Chyragov, *Russ. J. Coord. Chem.*, 2006, **32**, 304–308; (*d*) K. T. Mahmudov, M. N. Kopylovich and A. J. L. Pombeiro, *Coord. Chem. Rev.*, 2013, **257**, 1244–

1281; (*e*) K. T. Mahmudov, R. A. Aliyeva, S. R. Gadjieva and F. M. Chyragov, *J. Anal. Chem.*, 2008, **63**, 435–438.

8 (*a*) A. W. Addison, T. N. Rao, J. Reedijk, J. van Rijn and G. C. Verschoor, *J. Chem. Soc., Dalton Trans.*, 1984, 1349–1356; (*b*) K. Robinson, G. V. Gibbs and P. H. Ribbe, *Science*, 1971, **172**, 567–570.

9 (*a*) A. J. L. Pombeiro, M. F. C. Guedes da Silva and M. A. N. D. A. Lemos, *Coord. Chem. Rev.*, 2001, **219–221**, 53–80; (*b*) M. E. N. P. R. A. Silva, A. J. L. Pombeiro, J. J. R. Fraústo da Silva, R. Herrmann, N. Deus, T. J. Castilho and M. F. C. Guedes da Silva, *J. Organomet. Chem.*, 1991, **421**, 75–90; (*c*) A. I. F. Venâncio, M. L. Kuznetsov, M. F. C. Guedes da Silva, L. M. D. R. S. Martins, J. J. R. Fraústo da Silva and A. J. L. Pombeiro, *Inorg. Chem.*, 2002, **41**, 6456–6467; (*d*) A. I. F. Venâncio, M. F. C. Guedes da Silva, L. M. D. R. S. Martins and A. J. L. Pombeiro, *Organometallics*, 2005, **24**, 4654–4665.

10 (*a*) G. B. Shul'pin, *C. R. Chim.*, 2003, **6**, 163–178; (*b*) G. B. Shul'pin, Y. N. Kozlov, L. S. Shul'pina, A. R. Kudinov and D. Mandelli, *Inorg. Chem.*, 2009, **48**, 10480–10482; (*c*) G. B. Shul'pin, Y. N. Kozlov, L. S. Shul'pina and P. V. Petrovskiy, *Appl. Organomet. Chem.*, 2010, **24**, 464–472; (*d*) G. B. Shul'pin, *J. Mol. Catal. A: Chem.*, 2002, **189**, 39–66.

11 (*a*) A. M. Kirillov, M. V. Kirillova and A. J. L. Pombeiro, *Coord. Chem. Rev.*, 2012, **256**, 2741–2759; (*b*) L. M. D. R. S. Martins and A. J. L. Pombeiro, in *Advances in Organometallic Chemistry and Catalysis*, ed. A. J. L. Pombeiro, Wiley–VCH, Weinheim, 2013, ch. 22, pp. 285–294; (*c*) L. M. D. R. S. Martins and A. J. L. Pombeiro, *Coord. Chem. Rev.*, 2014, **265**, 74–88; (*d*) M. N. M. Milunovic, L. M. D. R. S. Martins, E. C. B. A. Alegria, A. J. L. Pombeiro, R. Krachler, G. Trettenhahn, C. Turta, S. Shova and V. B. Arion, *Dalton Trans.*, 2013, **42**, 14388–14401; (*e*) M. Sutradhar, M. V. Kirillova, M. F. C. Guedes da Silva, L. M. D. R. S. Martins and A. J. L. Pombeiro, *Inorg. Chem.*, 2012, **51**, 11229–11231; (*f*) T. F. S. Silva, L. M. D. R. S. Martins, M. F. C. Guedes da Silva, M. L. Kuznetsov, A. R. Fernandes, A. Silva, S. Santos, C.-J. Pan, J.-F. Lee, B.-J. Hwang and A. J. L. Pombeiro, *Chem.–Asian J.*, 2014, **9**, 1132–1143; (*g*) T. F. S. Silva, M. F. C. G. Silva, G. S. Mishra, L. M. D. R. S. Martins and A. J. L. Pombeiro, *J. Organomet. Chem.*, 2011, **696**, 1310–1318.

12 K. Weissermel and H. J. Arpe, in *Industrial Organic Chemistry*, VCH Press, Weinheim, 2nd edn, 1993.

13 M. V. Kirillova, Y. N. Kozlov, L. S. Shul'pina, Q. Y. Lyakin, A. M. Kirillov, E. P. Talsi, A. J. L. Pombeiro and G. B. Shul'pin, *J. Catal.*, 2009, **268**, 26–38.

14 (*a*) R. R. Fernandes, J. Lasri, A. M. Kirillov, M. F. C. Guedes da Silva, J. A. L. Silva, J. J. R. Fraústo da Silva and A. J. L. Pombeiro, *Eur. J. Inorg. Chem.*, 2011, 3781–3790; (*b*) R. R. Fernandes, J. Lasri, M. F. C. Guedes da Silva, J. A. L. da Silva, J. J. R. Fraústo da Silva and A. J. L. Pombeiro, *J. Mol. Catal. A: Chem.*, 2011, **351**, 100–111.

15 M. Peixoto de Almeida, L. M. D. R. S. Martins, S. A. C. Carabineiro, T. Lauterbach, F. Rominger, A. S. K. Hashmi, A. J. L. Pombeiro and J. L. Figueiredo, *Catal. Sci. Technol.*, 2013, **3**, 3056–3069.

16 (*a*) *APEX2 & SAINT*, Bruker AXS Inc., Madison, WI, 2004; (*b*) G. M. Sheldrick, *Acta Crystallogr., Sect. A: Found. Crystallogr.*, 2008, **64**, 112–122; (*c*) L. J. Farrugia, *J. Appl. Crystallogr.*, 1999, **32**, 837–838; (*d*) A. L. Spek, *Acta Crystallogr., Sect. A: Found. Crystallogr.*, 1990, **46**, C34.

